© 1969 IEEE. Personal use of this material is permitted. However, permission to reprint/republish this material for advertising or promotional purposes or for creating new collective works for resale or redistribution to servers or lists, or to reuse any copyrighted component of this work in other works must be obtained from the IEEE.

A LASER-INDUCED COMPTON BACK-SCATTERED PHOTON BEAM AT THE CAMBRIDGE ELECTRON ACCELERATOR*

Jon R. Sauer+, Richard H. Milburn and Charles K. Sinclair

Tufts University

and

Mircea Fotino

Cambridge Electron Accelerator

I. Introduction

The scattering of laser optical photons on extreme relativistic electrons has been proposed as a source of high-energy photon beams possessing both a high degree of polarization and a hard energy spectrum.[1,2,3,4] Early experiments at the Cambridge Electron Accelerator and elsewhere have demonstrated the feasibility of the method.[5,6,7,8] Recently, a multi-GeV short-spill "laser beam" has been achieved at the Stanford Linear Accelerator Center and is in routine use for exposures of the 82-inch hydrogen bubble chamber.[9] In the work described below, the beam of a normal-mode ruby laser was used at the CEA synchrotron to produce a long-spill "laser beam" with an intensity suitable for medium-energy counter experiments. The measured energy spectrum and the yield of these Compton back-scattered photons are in reasonable agreement with theoretical predictions.

The present results show that Compton scattering of a laser beam can be used for non-destructive probing of extreme-relativistic charged particle beams. The phase-space density distribution in the horizontal plane of the CEA internal beam was measured in this manner. The dependence of spatial charge distribution on machine energy, orbit perturbations, and time during the acceleration cycle was also determined. A particular application of this technique could be made to the analysis of storage-ring beams.

II. Experimental Apparatus and Procedures

Schematic diagrams of the experimental setup and the laser injection geometry are given in Fig. 1 and Fig. 2, respectively. The beam is brought into nearly head-on collision (3° crossing angle) with the CEA internal electron beam within an accelerator straight section. The two beams then undergo multiple crossings during successive revolutions of the electron beam. The back-scattered photon pulse is thus over 1 ms long. It is subsequently analyzed by a collimating system and counters. The size of the laser focal spot in the interaction region is determined by means of a stainless steel plate inscribed with a two-dimensional grid and mounted above the electron orbit at the interaction region. When the plate is lowered across the electron orbit, a few laser pulses produce on its surface, by local heating, a weld mark visible and measurable through the optical system. The preliminary alignment and calibration of the remotely-controlled laser-beam aiming mechanisms is thus accomplished.

The lasing medium is a 60°-cut Verneuil ruby, 6 5/8 in long and 3/8 in in diameter.[10] The front face is uncoated and the rear face anti-reflection coated to permit use of an external reflector in a 22 1/2 in long optical cavity. During normal operation at 1 pps and with input energies of about 2800 joules, new flashlamps yielded laser outputs in excess of 20 joules/pulse. With lamp aging, the laser output diminished to 10-12 joules/pulse. Typical lamp life was 25,000 to 40,000 firings. The laser produced light pulses up to 1.5 ms long, each consisting of many spikes about 1 μs long and spaced a few μs apart. The timing and relative intensity of the laser pulse were monitored through an interference filter by a photomultiplier viewing stray light within the laser housing. The total energy and spatial structure of the beam emerging from the laser were measured with an optical bolometer.[11] The light beam at the laser was oblong and irregular, typically about 0.180 in by 0.080 in, and its divergence in these two directions was 2.3 mrad and 4.5 mrad, respectively. The 60°-cut ruby yields linearly polarized light of relatively high purity, even in the absence of additional filtering. Measurements with an air-spaced Glan prism indicated the polarization in the present system to be greater than 70 percent.

The scattered photons emerge tangentially to the electron orbit and perpendicularly through a 0.002 in stainless steel window. They are detected by a total-absorption Cerenkov counter located about 10 m downstream from the interaction region (Fig. 1). The counter consisted of a square array of four identical lead glass blocks, each 8 cm x 8 cm and 23 X_0 long. Each block is viewed by a photomultiplier and the four outputs are mixed into a common signal. The beam entering the counter was filtered by an iron plate, 1/8-in thick, to remove the synchrotron and low-energy bremsstrahlung radiation. The output from the Cerenkov counter was gated to overlap the laser light pulse in order to minimize the background noise prevalent in the vicinity of the accelerator. The resolution of the Cerenkov counter is about 60%.

The experiment was operated primarily on a parasitic basis using only one pulse in each 64 from the 60 Hz CEA. The effects of beam instabilities, energy dispersion, and background from beam spillage were minimized by means of a late RF turn-off, and elimination of superfluous orbit distortions. Since the location of the electron orbit could change with accelerator operating conditions,

the tangent to the electron orbit had to be determined before each data run. This was accomplished by horizontal scanning with a 1/4 in slit across the front of the Cerenkov counter to locate the maximum of the bremsstrahlung from residual gas in the synchrotron straight section chamber. Equivalentally, a scan with the same slit could detect a minimum in the synchrotron radiation from the accelerator (Fig. 1). This minimum also corresponds to the straight portion of the electron orbit, and thus coincides with the bremsstrahlung maximum.

Figure 3 illustrates the profile of the typical back-scattered photon beam as measured by a horizontal scan. The discriminator level was set at 300-350 MeV below which the low-energy bremsstrahlung peak becomes predominant. The residual background is seen to be small, resulting in a good signal-to-noise ratio.

III. Laser Beam Results

The back-scattered photons have an energy distribution differing strongly from that of bremsstrahlung in that it is significantly enhanced at the high energy end. The peak energy is roughly proportional to E^2_{el}. For CEA electrons of maximum energy 6 GeV, and 1.79 eV optical photons, the "laser beam" spectrum extends up to 848 MeV. When observed at moderate laser and electron beam intensities, the energy spectra of the back-scattered photons are in qualitative agreement with theoretical predictions (Fig. 4). The effects of the Cerenkov counter's energy resolution and the accepted band of electron energies have been folded into the Klein-Nishina formula to produce the indicated theoretical spectrum. At high electron currents and light intensities, it is difficult to resolve individual back-scattered photons in the detector as the counter output exhibits pulse pile-up. It is therefore difficult to determine the maximum yields by means of direct photon counting techniques. This phenomenon also distorts measured pulse-height spectra since several high-energy photons accumulate in a time shorter than the resolving time (200 ns) of the analyzing system. The actual efficiency of the achieved interaction process is thus inferred from measurements made at reduced electron currents and laser intensities.

Using known geometry of the laser optical system and the experimentally determined values of the laser beam and electron beam cross sections, the calculated back-scattered photon yield integrated over the entire energy spectrum[4] is 90-95 photons/mA(electron beam)-joule(laser pulse). The measured yield was typically 30-45 photons/mA-joule. These results can be considered as quite consistent in view of the approximations made in the rate calculation and the probable but unknown losses due to vignetting in the optical system. Extrapolating these yields to 15 mA and 15 joules, as are routinely possible with the CEA and the present laser system, one probably obtained actual rates up to 6000-10,000 photons per second.

IV. Accelerator Beam Results

The laser beam technique was also studied as a non-destructive probe of the electron beam structure. After initial alignment, horizontal scans with both the laser beam and the slit could be taken in minutes, with good reproducibility. Laser scans across the electron beam, which sample the spatial electron density, were made under a variety of accelerator operating conditions and found to resolve orbit displacements and horizontal cross section changes down to 0.010-0.020 in. Slit scans, such as shown in Fig. 3, resolved 0.050 in at the counter, or angles of less than 0.2 mrad.

The system was designed to maximize the volume overlap of electron and light beams in order to obtain as many photons as possible at the Cerenkov counter. However, since the signal-to-noise ratio obtained was very satisfactory, it was possible to stop down the laser focal spot size, and to reduce the scanning slit aperture to 1/16 in in order to improve the resolving power of the system. The laser stop, placed just beyond lens L1 in Fig. 2, reduced the diameter of the laser beam focus in the interaction region to about 1/5 of the electron beam width. It was then possible to map out the data required to infer the density distribution in the horizontal projection of electron beam phase space. The family of curves shown in Fig. 5 was generated by horizontal scans with the 1/16 in slit, at various fixed laser spot positions. A linear correlation was observed between the laser spot positions and the maxima of these curves, from which one may infer the slope of the line passing through the set of points x_{max} on the horizontal phase ellipses.[12] A similar family of curves from scans with the laser spot, at various slit positions, leads to a measurement of the slope of linear locus connecting the points x'_{max}. From the first family of curves, and from interpolating the measured absolute yields of back-scattered photons, one can map out the equi-density contours. Such a family and the computed loci of extremals are shown in Fig. 6. A preliminary analysis shows that these results are in rough quantitative agreement (35 percent) with CEA orbit calculations based upon the magnetic field distribution in the accelerator.

V. Conclusions

These results represent the continuation of work initiated at CEA in 1964 with the detection of back-scattered laser photons.[5] It is shown that it is possible to obtain such photon beams at intensities practical (10^3-10^4/s) for use in those high-energy experiments in which relatively low intensities are compensated by a high and controllable polarization and by a harder energy spectrum. Recent advances in laser technology could increase the yield one and perhaps two orders of magnitude.[13]

The applicability of the laser beam as a non-destructive probe for relativistic beam studies has been demonstrated. A more versatile system designed specifically as a beam probe could achieve considerably better space and time resolutions in both horizontal and vertical projections. Such a system would require no special orbit distortions, no disturbing magnetic fields, and would remove only a negligible fraction of the beam particles. It might prove appropriate for quantitative beam studies in storage rings, particularly at locations relatively inaccessible by other methods.

Acknowledgements

We thank Prof. K. Strauch, and also H. Winick, J. Hagopian, H. Mieras, and K. Robinson of CEA for their special assistance to this project.

References

*Supported by the U.S. Atomic Energy Commission.

+U.S. Steel Fellow during 1966-1968.

[1]Richard H. Milburn, Phys. Rev. Letters 10, 75 (1963).

[2]F. R. Arutyunian and V. A. Tumanian, Phys. Letters 4, 176 (1963).

[3]F. R. Arutyunian, I. I. Goldman and V. A. Tumanian, Zh. Eksper. Teor. Fiz. 45, 312 (1963) translation: Soviet Physics JETP 18, 218 (1964).

[4]Richard H. Milburn, SLAC Report No. 41, May 1965.

[5]C. Bemporad, R. H. Milburn, N. Tanaka and M. Fotino, Phys. Rev. 138B, 1546 (1965).

[6]O. F. Kulikov, Yu. Ya. Telnov, E. I. Filippov and M. N. Yakimenko, Phys. Letters 13, 344 (1964).

[7]O. F. Kulikov, Yu. Ya. Telnov, E. I. Filippov and M. N. Yakimenko, Pribory i Tekhnika Eksperimenta, No. 4, 14 (1967).

[8]Kulikov et al., Lebedev Institute Preprint No. 170, Moscow 1968.

[9]C. K. Sinclair, J. J. Murray, P. R. Klein, and M. Rabin, paper I-24 in these Proceedings.

[10]Adapted from a Raytheon LH8 laser head and LPS-21A power supply, with a closed-circuit water cooler permitting operation at 1 Hz. Pumping was by a single FX 47B - 6.5 lamp mounted in a silvered elliptical cavity.

[11]A TRG Model 108 bolometer, provided with a graphite aperture plate.

[12]See, for example, Steffen, High Energy Beam Optics, Interscience, 1965.

[13]R. H. Milburn, Proc. Sixth Int. Conf. on High-Energy Accelerators, 1967, Cambridge, Mass., p. A-158.

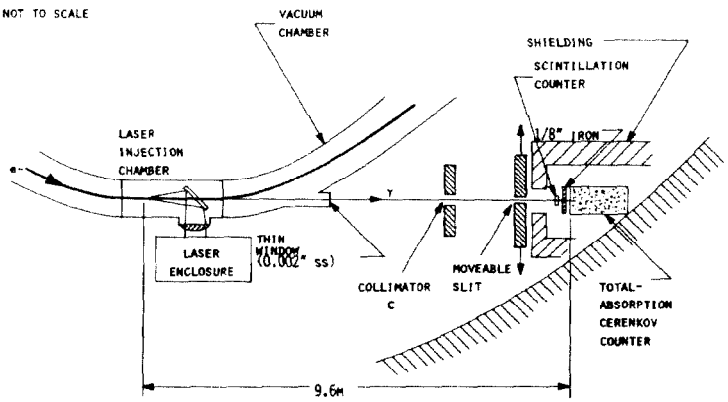

Fig. 1 (left). Schematic Diagram of Experimental Setup.

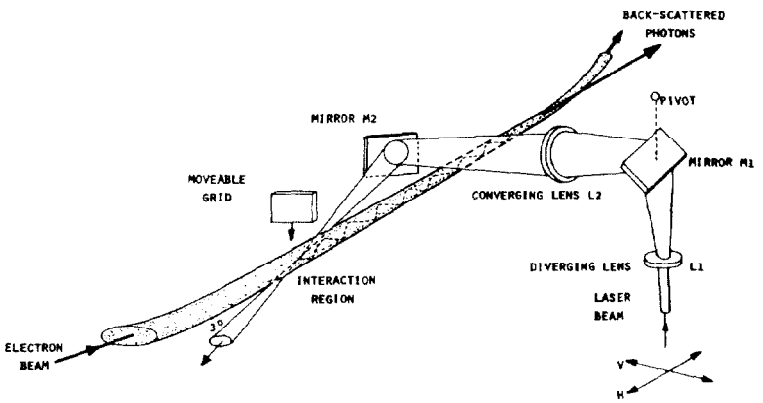

Fig. 2 (right). Laser Injection Geometry.

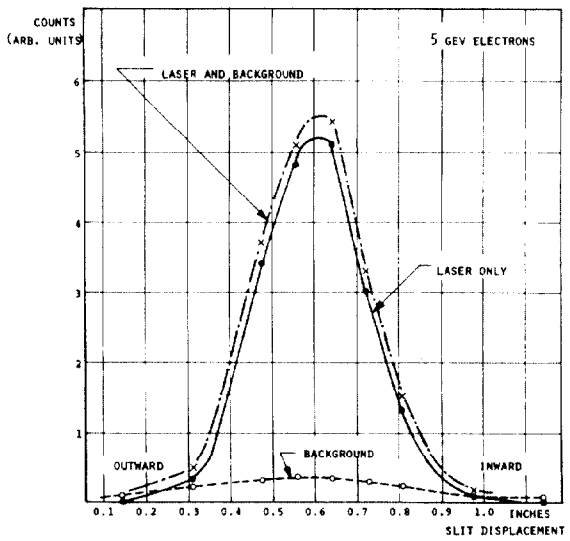

Fig. 3. Slit Scan at Cerenkov Counter Entrance.

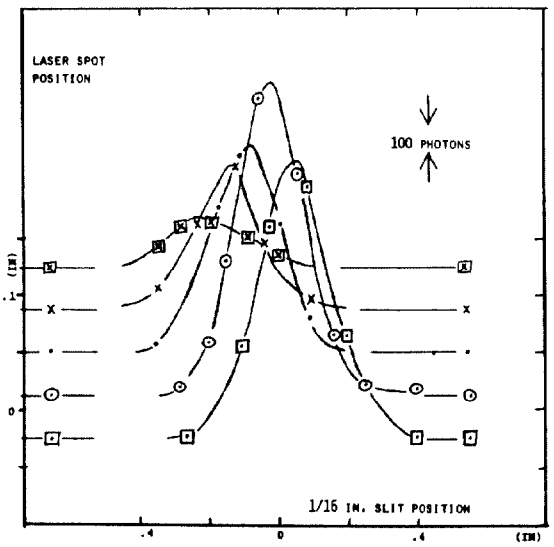

Fig. 5. Horizontal Slit Scans at Various Fixed Laser Positions.

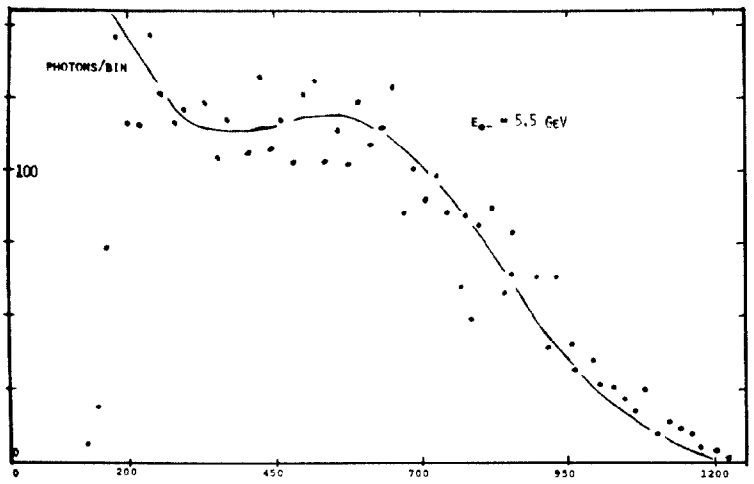

Fig. 4. Theoretical and Observed Spectrum.

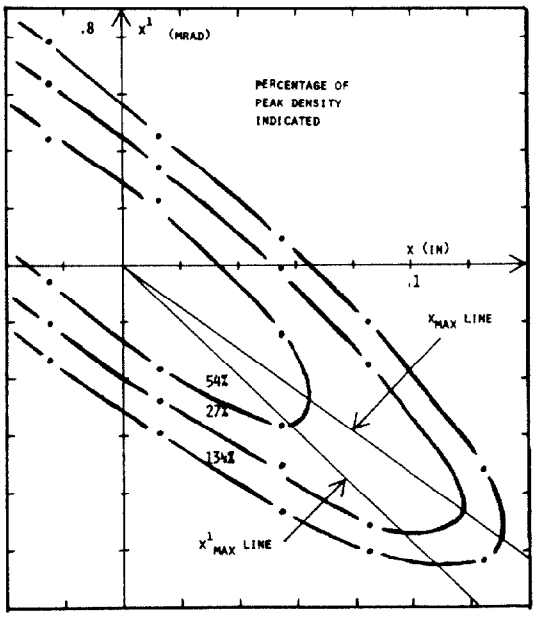

Fig. 6. Phase Plane Equi-Density Contours.